ARTHROPOD SYSTEMATICS & PHYLOGENY

73 (3): 477 – 488
23.12.2015

SENCKENBERG

Functional morphology of the mandibular apparatus in the cockroach *Periplaneta americana* (Blattodea: Blattidae) – a model species for omnivore insects

Tom Weihmann *[1], Thomas Kleinteich[2], Stanislav N. Gorb[2] & Benjamin Wipfler *[3]

[1] Insect Biomechanics Group, Dept. of Zoology, University of Cambridge, Downing Street, Cambridge CB2 3EJ, UK; Tom Weihmann * [tw424@cam.ac.uk] — [2] Functional Morphology and Biomechanics Group, Kiel University, Am Botanischen Garten 9, 24118 Kiel, Germany — [3] Entomology Group, Institut für Spezielle Zoologie und Evolutionsbiologie mit Phyletischem Museum, Friedrich-Schiller-Universität Jena, Erbert Str. 1, 07743 Jena, Germany; Benjamin Wipfler * [benjamin.wipfler@uni-jena.de] — * Corresponding author

Accepted 30.ix.2015.
Published online at www.senckenberg.de/arthropod-systematics on 14.xii.2015.

Editor in charge: Frank Wieland.

Abstract

We examine the functional morphology of the mandibular apparatus, including its driving muscles, of the generalist insect *Periplaneta americana* using a combination of μ-computed tomography and geometrical modelling. Geometrical modelling was used to determine the changes of the mean fibre angle and length in the mandibular adductor muscle over the physiological range of mandible opening. The roughly scissor-like mandibles are aligned along the dorso-ventral axis of the head and are characterised by sharp interdigitating distal teeth, as well as a small proximal molar region. The mechanical advantage of the mandibles, i.e. the ratio between inner and outer levers, ranges between 0.37 to 0.47 depending on the considered incisivus. The mandibular abductor muscle is comprised of eight muscle fibre bundles, which are defined by distinct attachment positions on the sail-like apodeme protruding from the medio-lateral basis of the mandibles into the head lumen. Compared to carnivorous, herbivorous, or xylophagous insects, the relative volumes of the mandibular abductor and adductor muscle are small. Dependent on the mandible opening angle, the mean fibre angle of the adductor muscle ranges from 34° to 21°, while mean fibre length changes from 1.24 mm (closed mandible) to 1.93 mm at maximum mandible opening. Many of the specific morphological features found in the chewing apparatus of *P. americana*, such as the presence of a mola in combination with distal incisivi, small relative muscle size and the intermediate fibre angle can be understood as adaptations to its omnivorous life style.

Key words

Comparative morphology, insect, head, mouth parts, skeleton, muscles, mandibles, biting, chewing.

1. Introduction

Insects are the largest group of organisms in terms of species number (Grimaldi & Engel 2005) and provide a major part of the animal biomass. Although they are in the focus of attention of many organismic biologists, there still remain many functional aspects that are sparsely studied. One of these aspects is the physiology of ingestion and food processing. With the dawn of the μ-computed tomography (μ-CT) technique, internal muscle architecture has become increasingly widely used for phylogenetic analyses (e.g. Friedrich et al. 2014; Wipfler et al. 2015). However, since most morphological studies rely on individual specimens, they largely disregard intraspecific variation and specific ontogenetic adaptations. Even if mean values and measures of dispersion were

provided, anatomical description alone does not provide evidence to determine functional consequences of the muscles and associated skeletal arrangements and structure (Weihmann et al. in press). In particular, this holds for arthropods since physiological muscle properties are much more variable than in vertebrates (Jahromi 1969; Taylor 2000). Muscles, in turn, are the drivers of almost all animal movements. Their arrangement in the skeletal system, structure, and their physiological properties determine the movement capabilities of an animal. Muscle function and emerging capabilities of the powered limbs have decisive impact on the development, behaviour, interactions with the environment, and the evolution of species.

Locomotion, mating and food acquisition are biological functions that rely on muscle powered limbs, i.e. the typical arthropod mouthparts in the case of feeding. In many insects, specifically those with biting-chewing mouthparts, the paired mandibles are the strongest parts responsible for biting and reducing larger food items into smaller digestible pieces. Thus, they are indispensable for food acquisition, grinding, and intake. Alongside these key features, mandibles are also used for defence and aggression, digging, feeding nest mates or offspring, clinging, and transport (Chapman 1995; Clissold 2007).

The mechanics of neopteran insects' mandibles is relatively simple; they can be characterised as two class 3 levers working against each other (Clissold 2007). For each mandible, the driving forces are generated predominantly by a single adductor muscle and transmitted to teeth edges or grinding ridges at its distal parts. The adductor is attached to the median basis of the mandible and is antagonised by a much weaker abductor muscle attaching at the lateral basis of the mandible. In neopteran insects, the mandibles are connected to the head capsule via simple hinge joints, whose rotational axes are defined by anterior and posterior condyli (e.g. Snodgrass 1944; Paul 2001; Blanke et al. 2012). Therefore, a mandible can move only in a single plane. This makes the mechanics of the biting process (Schmitt et al. 2014) much simpler than for instance those of the flying or walking apparatuses (Maier et al. 1987; Ahn & Full 2002; Siebert et al. 2010). Therefore, the experimental and analytic effort is reduced, which also reduces the effort of future comparative studies leading to a better understanding of interactions between single parts of a whole functional unit.

Bite mechanics is largely underexplored in insects, and detailed morphological data including physiological examinations are notoriously rare. The largest body of literature deals with the biting physiology of the chelae of larger crustacean species, which comprise some of the strongest biters in the animal kingdom (Taylor 2000). Additionally, there are some papers about biting in some orders of the chelicerates (van der Meijden et al. 2012, 2013). However, in crustaceans, scorpions and solpugids, the structures responsible for strong biting are chelae or chelicerae. This is in stark contrast to insects where the driving muscles are not situated in these limbs but rather within the head capsule. Some papers deal with the functional morphology and neuronal control of mandible movements in insects (Gorb & Beutel 2000; Paul & Gronenberg 2002; Li et al. 2011), but only few studies focused on the determination of bite forces. Wheater & Evans (1989) examined maximum bite forces and mandible closer size in several ground and rove beetles. Goyens et al. (2014) recently measured bite forces of stag beetles. The carnivorous ground beetles exhibit specialized predatory mandibles while the stag beetles' enlarged mandibles are used primarily in male–male fights for mating opportunities and not for food processing.

As a first step to a more general understanding of insect biting, we examine the structure of the mandibles and associated muscles in the omnivore cockroach *Periplaneta americana*. A detailed examination of the head morphology and anatomy of this species is provided by Weissing et al. (in press). Schmitt et al. (2014) studied the movement of the mandible with in vivo X-ray radiography. In conjunction with the exerted voluntary bite forces of *P. americana*, which were studied by Weihmann et al. (2015), here we provide a detailed study of insect biting relying on anatomical and physiological data from eight specimens. We analysed fibre angles and lengths of the major fibre bundles of six mandibular adductor muscles (m. craniomandibularis internus (0md1)) and provide the relative sizes of adductor and abductor muscles (m. craniomandibularis externus posterior (0md3)) of seven other hemimetabolous insect species from four different insect orders. Moreover, the results for these omnivore, xylophage, carnivore, and herbivore species are compared with the conditions found in *P. americana*. Finally, we draw inferences on the functioning of biting-chewing mouthparts of insects in general, and compare it with those of crustacean chelae and chelicerae of solpugids.

2. Methods

The present study is based on eight adult specimens of *Periplaneta americana*. They originated from a laboratory colony at the Institut für Spezielle Zoologie und Evolutionsbiologie of the Friedrich-Schiller-Universität Jena, Germany. The colony exists since 2012 and was originally derived from professionally bred animals (available at: www.schaben-spinnen.de). The animals were kept at room temperature (23–25°C) in perspex cages and fed twice a week with porridge oats; water was provided *ad libitum*. The animals used in the present study had a mean body mass of 1.12 ± 0.17 g. The same animals were previously examined with respect to the voluntary bite forces (Weihmann et al. 2015). With these experiments we also determined the opening range of the mandibles. Voluntary opening angles ranged from 46° to about 100°, with the former meaning completely closed mandibles, i.e. the condition used for µ-CT-examinations

(see below). Despite the much larger range of voluntary movements, significant bite forces were obtained only between 55° and 85° of mandible opening. At angles smaller than 55° the interactions of the two mandibles with the force sensor hampered further mandible closure and therefore the measurement of reliable force values. At angles larger than 85° passive forces of the joint structure dominates mandible closing (see Weihmann et al. 2015). After measuring the biting forces, the animals were decapitated immediately and killed by freezing (–18°C) for several minutes. Afterward we transferred them to 70% ethanol.

The opening angle of a mandible was defined as the angle between the horizontal line, and the length axis of a mandible (oa; Fig. 1E). The length axis of a mandible, in turn, was defined as the line from the anterior condyle of the mandible joint to the tip of the distal most tooth (ma; Fig. 1E). Both measures, horizontal line and mandible axis, were acquired from video recordings, which occurred synchronously with the force measurements. During the process of filming, the labrum was folded up and fixed, to guarantee a clear view on the mandibles.

The system of coordinates was aligned individually. Thus, the horizontal plane was spanned by the joint axes of the left and right mandible joints with the connecting line between the two anterior condyles defining the horizontal axis of the head (Fig. 1A,D). The transverse plane was defined by these condyles and was always perpendicular to the horizontal plane. The sagittal plane, in turn, subtends the horizontal plane along the centreline between the anterior condyles and is perpendicular to both, the horizontal and the transverse plane. The intersection line of the horizontal and the sagittal planes also defines the length axis of a cockroach's head.

For µ-computed tomography (µ-CT), the heads of the specimens were dried with hexamethyldisilazane and mounted on a sample holder. The scans were performed on a Skyscan 1172 (Bruker, Kontich, Belgium) that was operated at an acceleration voltage of 40 kV and a current of 250 µA. The exposure time for a single x-ray image was 720 ms; x-ray projections were captured over a full 360° rotation of the specimen at steps of 0.130°. The x-ray images were then converted into a volumetric data set that consisted of isometric voxels with a voxel size of 3.07 µm. This volumetric µ-CT data (Fig. 1C) was analysed with Visage Imaging Amira 5.2.2 (Visageimaging, San Diego, USA) using the length and volume measurement tools. Illustrated volume renders were implemented with VG Studiomax 2.2 (Volume Graphics GmbH, Heidelberg, Germany). The µ-CT scans are deposited in the collection of the Phyletisches Museum in Jena, Germany (scans 4–12 in Polyneoptera / Blattodea / Periplaneta americana).

All morphological and anatomical measures were taken from the 3D data provided by the µ-CT scans. The general morphological terminology follows Seifert (1995) and for the musculature Wipfler et al. (2011). For each specimen, we determined characteristic measures of both mandibles. These measures were the positions of the anterior and posterior condyles, the attachment position of the adductor tendon to the mandible base and the positions of the mandible teeth. They were used to determine the respective distances to the joint axis, i.e. the lengths of the inner and outer levers, and to determine the angles between them (Fig. 1E). Thereby, the lengths of the inner and outer levers were defined as the distances of the teeth, or the attachment of the adductor tendon, perpendicular to the joint axis (Fig. 1E, Table 3). The effective inner lever, which is pivotal for the efficiency of the force transmission, was defined as the length of the projection of the line between the joint axis and the tendon attachment point onto the horizontal line (Fig. 1E). Despite immediate transfer to ethanol, only three specimens (1.16 ± 0.1 g) had sufficiently well preserved fibres of the adductor muscle for further examination. From these three specimens we examined the left and the right mandibular adductor and abductor muscles.

We distinguished eight distinct compartments in the mandibular adductor muscle (m. craniomandibularis internus), which are defined by their origin on the tendon (Fig. 2). The abductor muscle (m. craniomandibularis externus posterior) is much smaller and does not divide into different compartments. Fibre length and fibre angle of five muscle fibres that were evenly distributed in the bundle were determined for each of the eight major compartments of the adductor and for the abductor. We selected one fibre in the centre of the bundle and four close to the end points of the defining axes of the roughly elliptic cross section of the fibre bundles. Additionally, we measured the effective cross sectional area of the eight compartments of the adductor and that of the abductor at their widest parts, i.e. we determined the area of an elliptic envelope of virtual sections perpendicular to the predominant fibre orientation with the length measuring tool of Visage Imaging Amira 5.2.2. The fibre angles were determined with respect to the major direction of the muscle force (mf-fa; Fig. 1E,F), which was defined as the direction from the attachment point of the tendon at the mandible base to the centre point of a muscle's attachment area at the head capsule. The mean values of fibre length and angles were calculated individually for each fibre bundle and weighted according to the relative contribution of the single bundles to the total cross section area of a mandibular adductor. In this way, the mean fibre length and angle of the mandible adductor were determined individually for the positional conditions during µ-CT imaging at which mandibles were closed, i.e. with maximally shortened adductor muscles. Muscle length changes and angular changes, then, were calculated based on these weighted means averaged across all examined specimens.

The position of the tendon attachment changes when a mandible rotates around its pivot axis. Depending on the length of the inner lever and the opening angles of the mandibles, dorso-ventral and lateral displacements were determined (see results), which led to corresponding length changes and angular changes of the muscle fibres. Potential length changes of the tendon are negli-

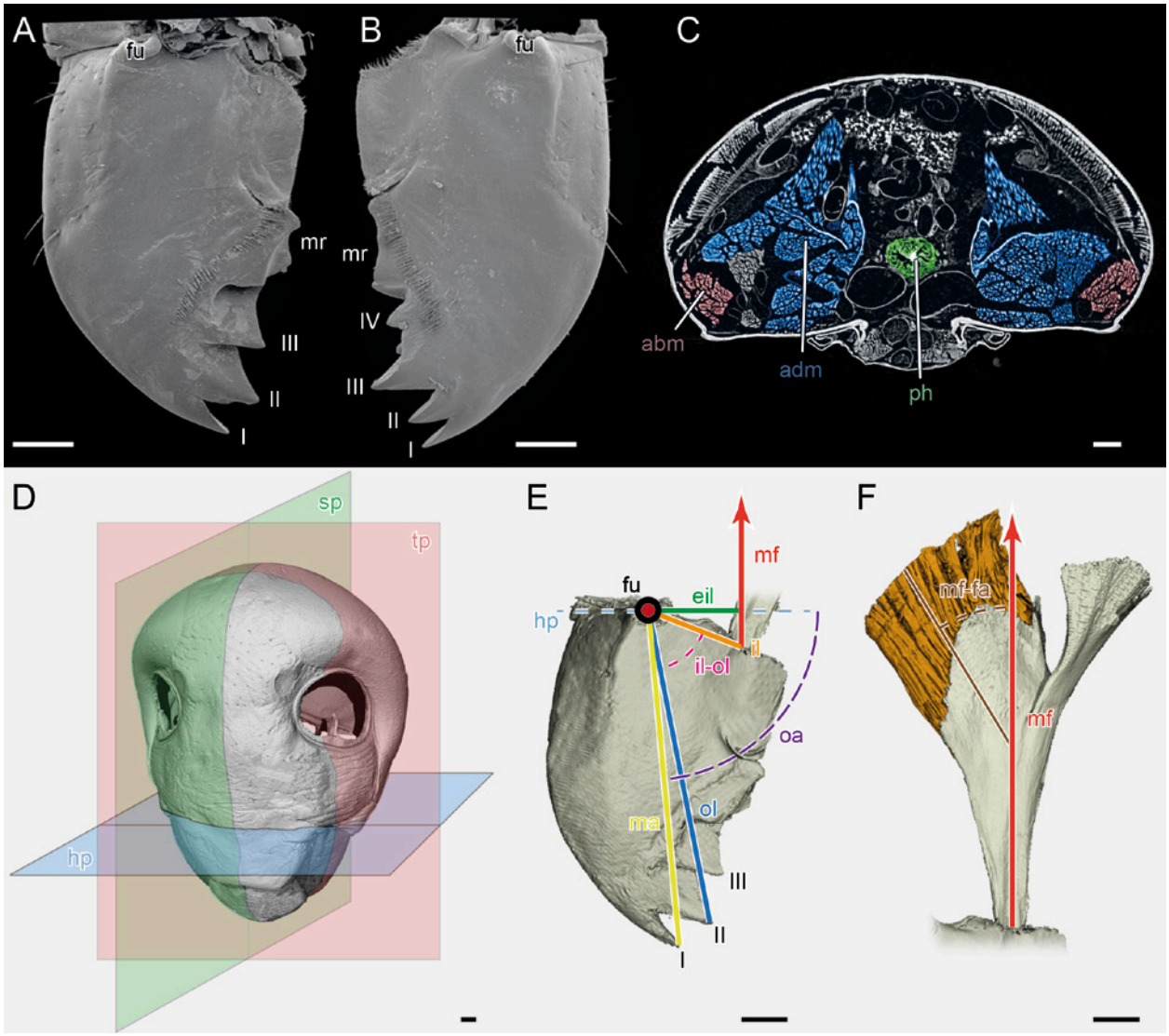

Fig. 1. A: right mandible of *Periplaneta americana* in anterior view; **B**: left mandible of *Periplaneta americana* in anterior view; **C**: µ-computed tomographical section of the head capsule; mandibular adductor muscle in blue, mandibular abductor muscle in red, pharynx in green; **D**: coordinate system of the head capsule; **E**: distances, points and angles on the mandible; **F**: angles and directions on the mandibular tendon. — ***Abbreviations***: I–IV: incisivi; abm: mandibular abductor muscle; adm: mandibular adductor muscle; eil: effective inner lever; fu: fulcrum; hp: horizontal plane; il: inner lever; il-ol: angle between outer and inner lever for the 2nd incisivi; mf: main direction of muscle force; ma: mandibular axis or outer lever of the 1st incisivus; mf-fa: angle between the main direction of the muscle force and one muscle fibre; mr: mandibular molar region; oa: opening angle of the mandible; ol: outer lever of the 2nd incisivi; ph: pharynx; sp: sagittal plane; tp: transverse plane. Scale bars: 0.5 mm.

gible as insect tendons usually are about 40 times stiffer than those of vertebrates (BENNET-CLARK 1975; KER et al. 1988). Since lateral displacements were only about 0.3 mm and small compared to the total length of the muscle tendon system of about 3.8 mm (see results), their impact on the fibre length and angle changes is negligible. Thus, calculations of the mean fibre length change and mean angle change rely only on displacements in dorso-ventral direction (see results section). By applying this dorso-ventral displacement on the mean fibre length and angle, length and angular changes were calculated as changes in a right-angled triangle with the lengthening leg lying onto the major direction of the muscle force (cp; Fig. 1E,F). For the calculation of the fibre length changes, i.e. those of the hypotenuse, the Pythagorean theorem was applied. Angular changes were calculated accordingly as changes in the angle between the leg of the right-angled triangle in parallel with the main force direction and the hypotenuse by using trigonometric functions. All lengths, angles, changes, and statistics were calculated with MATLAB R2010a (The MathWorks, Natick, MA, USA). All variance in measurements is standard deviation (mean ± s.d.).

Muscle and head capsule volumes of *P. americana* were measured with the volume measure tool of Amira 5.2.2. The volume of the head capsule included the mouthparts and eyes but not the antenna. The volume of the muscles includes the respective tendon. These val-

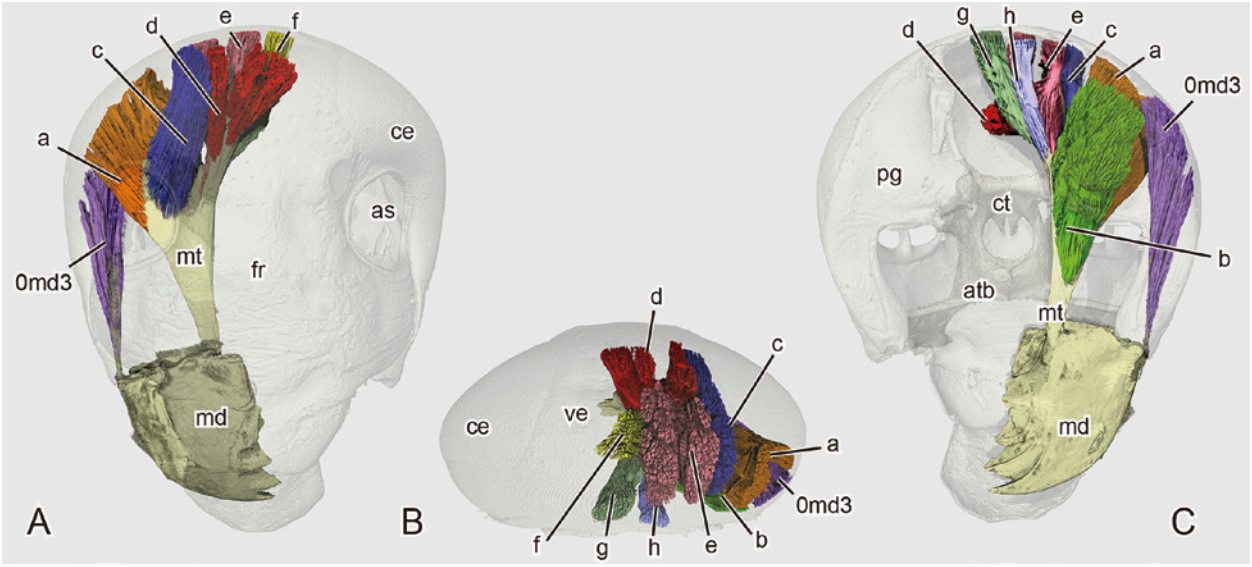

Fig. 2. Bundles of the right mandibular adductor muscle (m. craniomandibularis internus, 0md1) and abductor muscle (m. craniomandibularis externus posterior, 0md3) of *Periplaneta americana*, 3D-reconstruction based on µ-computed tomography. **A**: frontal view; **B**: dorsal view; **C**: posterior view. — ***Abbreviations***: 0md3: M. craniomandibularis externus posterior; a–h: bundles of M. craniomandibularis internus; as: antennal socket; atb: anterior tentorial bridge; ce: compound eye; ct: corpotentorium; fr: frons; md: mandible; mt: tendon of M. craniomandibularis internus; pg: postgena; ve: vertex.

ues were also measured for other polyneopteran lineages with different diets, for which µ-CT scans of the head were available in the collection of the Phyletisches Museum, Jena, Germany: the xylophagous termite *Mastotermes darwiniensis* and cockroach *Salganea* sp., the omnivorous roach *Ergaula* sp., the insectivorous mantid *Hymenopus coronatus* (Wipfler et al. 2012) and grylloblattodean *Galloisiana yuasai* (Wipfler et al. 2011) as well as the herbivorous phasmatodeans *Phyllium siccifolium* (Friedemann et al. 2012) and *Timema* sp. (one individual studied respectively).

3. Results

3.1. Mandibular morphology

In the resting position, the mandibles of *P. americana* are oriented along the dorso-ventral axis. Thus, comparable to scissor blades, they act as a pair of sharp cutting edges moving closely past each other, allowing shearing of tough materials. In contrast to scissors, however, each mandible has its own pivot and their axes are tilted towards each other. On average the angles between the joint axes and the sagittal plane were about 17 ± 2°, with the posterior condyles positioned more laterally than the anterior ones.

The teeth of the mandibles intercalate with each other, and thus left and right mandibles have to be slightly unsymmetrical. The left mandible has four distal teeth while the right has only three teeth. The distances of the teeth towards the joint axes vary (Table 3), but the distances from the distal-most teeth to the joint axes are both about 2.52 mm (± 0.13 in the right and ± 0.10 in the left mandible) and do not differ significantly from each other (t-test, p = 0.34). The distances from the joint axes to the 3rd left and 2nd right teeth were 2.33 ± 0.11 mm and 2.32 ± 0.10 mm, respectively, which was also very similar (p = 0.95). The teeth have different shapes; particularly the 3rd left and 2nd right teeth are characterised by sharp proximal edges. With closed mandibles the length of the muscle tendon complex of the mandibular adductor was 3.8 mm ± 0.16 mm (i.e. the length from the attachment of the tendon at the mandible base to the centre point of the muscle attachment area at the head capsule).

3.2. The morphology of the mandibular adductor muscle and its tendon

In *P. americana* the mandibular adductor tendon is an elongate structure with varying degrees of sclerotization. It is attached on the mesal basal edge of the mandible. This articulation zone is not sclerotized and therefore highly flexible. However, manual testing showed that in alcohol preserved specimens the apodemes' material is denatured and conveys the impression of high resilience to bending which is not the case in fresh specimens. From this articulation, in the frontal view, the tendon continues as a roughly triangular, sail-like, planar structure into the lumen of the head capsule (Fig. 2). Close to the mandibular articulation the basal wing of the tendon is located on the lateral side of the tendon. Both disto-mesal and disto-lateral wings are attached distally (see also fig. 11 in Weissing et al. in press).

In both hemispheres of the head of all studied speci-

Table 1. Origins at the mandible apodeme and insertions at the head capsule of the mandible closer bundles (M. craniomandibularis internus) in *Periplaneta americana*.

Bundle	Origin	Insertion	Comment
a	laterally on the distal part of the basal wing and the entire lateral wing	latero-posterior vertex	the most lateral bundle
b	along the entire ventral surface of the basal wing of the mandibular tendon	postgena, laterad the foramen occipitale	a broad bundle
c	mesal side of the lateral wing of the tendon	along the entire antero-posterior vertex, mesal to bundle a and laterally of d and e	the biggest bundle
d	posterior edge of the mesal wing of the tendon	anterior vertex, mesal to bundle c; in the right hemisphere with two dinstinct subcomponents while the left hemisphere has only one. The additional mesal subcomponent of the right bundle attaches in the midsagittal area, anterior to bundle f of the left hemisphere.	forms a column with bundle e
e	along the entire lateral side of the mesal wing of the tendon	posterior vertex, mesal to bundle c and lateral of bundles g and f, directly posterad bundle d. In the right hemisphere with two distinct subcomponents, in the left one with only one.	forms a column with bundle d
f	posterio-mesal edge of the mesal wing of the tendon	anterio-mesal vertex	the most anterior bundle of the mesal row
g	mesal side of the mesal wing of the tendon	mesally on the vertex, posterior to bundle f and anterior to bundle h	the mesal bundle of the mesal row
h	ventro-mesal edge of the mesal wing of the mandibular tendon	mesally on the dorsal edge of the foramen occipitale	the thinnest bundle of the muscle

Table 2. Fibre lengths, fibre angles, cross section areas (in mm^2 and % of the entire muscle) and volume (in mm^3 and % of the entire muscle) of the eight muscle fibre bundles of the mandibular adductor of *Periplaneta americana*.

bundle	length [mm]		angle [°]		area [mm^2]		area [%]		volume [mm^3]		volume [%]	
	mean	std	mean	std	mean	std	mean	std	mean	std	mean	std
a	1.17	±0.18	30.30	±6.0	0.53	±0.05	23.90	±2.6	0.78	±0.09	24.78	±2.53
b	1.17	±0.19	39.70	±5.9	0.50	±0.08	22.50	±2.3	0.62	±0.11	19.39	±1.46
c	1.52	±0.25	41.90	±15.3	0.33	±0.05	14.70	±2.4	0.60	±0.15	18.62	±3.18
d	1.00	±0.05	59.80	±5.7	0.21	±0.06	9.30	±2.1	0.23	±0.10	6.93	±2.31
e	1.34	±0.23	11.00	±7.6	0.38	±0.14	17.20	±6.5	0.60	±0.25	18.59	±5.06
f	1.11	±0.1	41.60	±14.1	0.13	±0.05	5.70	±2.2	0.16	±0.04	5.03	±1.44
g	1.25	±0.08	26.40	±11.1	0.12	±0.04	5.20	±1.9	0.14	±0.05	4.79	±2.02
h	1.29	±0.15	30.60	±6.5	0.03	±0.01	1.50	±0.6	0.06	±0.02	1.87	±0.55

mens of *P. americana* the adductor can be divided into eight distinct compartments. These muscle fibre bundles have defined areas of origin on the mandibular tendon (Table 1; Fig. 2). In principle, the attachment of the mandibular adductor on the head capsule is fan-shaped, i.e. the attachment areas of the single fibre bundles are mostly oriented along the length axis and lined up along medio-lateral directions (Fig. 2). Only the bundles *b* and *h* deviate from this pattern and attach exclusively on the posterior wall of the head capsule. Although all bundles can be identified in both hemispheres, where they have the same origin on the tendon, the structure of some bundles differed consistently between the hemispheres. This difference is reflected by increased standard deviations of the cross-section areas (e.g. bundle *e* in Table 2). In two specimens, the right adductor seems to be somewhat larger than the left one; in the third specimen, however, it appears to be the opposite. Though the imbalances might be a consequence of the asymmetric dentition of right and left mandibles, deducing a general trend does not seem to be reasonable at this stage due to the small sample size. Therefore, we confined our analyses to the averages of left and right muscles of all three specimens (see below). Nevertheless, the issue with the mandibular asymmetry should be examined in more depth with larger sample sizes in the future.

3.3. Characteristic lengths and angles with closed and open mandibles

Subsequent to the straining physiological experiments and the preparation for the µ-CT scans, the resting position of the mandibles could be reliably identified only in two right and four left mandibles. The resultant position of the mandible base, i.e. the inner lever, was close to the horizontal line when mandibles were closed (right: −4.6 ± 1.1°; left: 0.1 ± 1.2°). The inner levers were about 0.92 mm in both mandibles (right: 0.92 ± 0.06 mm; left: 0.92 ± 0.09 mm). A rotation of this lever about the joint axis results in positional changes of the mandibles. Within the range of significant bite forces (55° to 85° of mandible opening), this change corresponds to a dorsoventral displacement of the tendon of about 0.45 mm. Changes from closed to maximally opened mandibles lead to a displacement of 0.7 mm. Since the orientation of the muscle changes only marginally with increasing mandible opening (see methods section) the effective lever, i.e. the horizontal distance between the pivot and the attachment of the tendon, reduces by about 30% when considering the range from closed to maximally open mandibles. If we consider those opening angles, where considerable bite forces were measured, i.e. from about 55° to 85°, the effective lever decreased by only 18%. Hence, the effective mechanical advantage (EMA), i.e. the quotient of the effective inner lever to the outer lever, changed too. The ratio of the distances between pivot and tendon attachment on the one side and pivot and the outer lever on the other side are constant and define the mechanical advantage (MA) of specific teeth. Depending on the tooth considered (Table 3), this ranged from 0.37 to 0.47. Here, the position of the 2nd right and 3rd left teeth seems to be of particular significance. Both teeth are well developed and their proximal rims are cutting edges; their MA is about 0.39.

Volumes and cross sectional areas of the eight fibre bundles differ strongly from each other, but their individual contributions to the cross sectional area of the whole muscle are relatively constant among the measured specimens (Table 2). On average the mandibular adductors had a cross sectional area of about 2.23 ± 0.24 mm^2. The bundles *a, b, c* and *e* were the largest fibre bundles making up about 78% of the whole muscles' cross sectional area (Fig. 2; Table 2), which was calculated by summing up the cross sectional areas of the single bundles. The mean weighted fibre angle is about 34° whereas single fibre bundles deviate markedly from this value (Table 2). The mean weighted fibre length was about 1.24 mm while the mean lengths of the single fibre bundles ranged from 1 to 1.52 mm.

When the cockroach mandibles open, the length of the effective inner lever, the mean fibre length, and the mean fibre angle change markedly (Fig. 1E,F). Starting from closed mandibles the mean fibre angle decreases from about 34° to about 21° at maximally opened mandibles (Fig. 3). At mandible opening from 55° to 85°, the mean

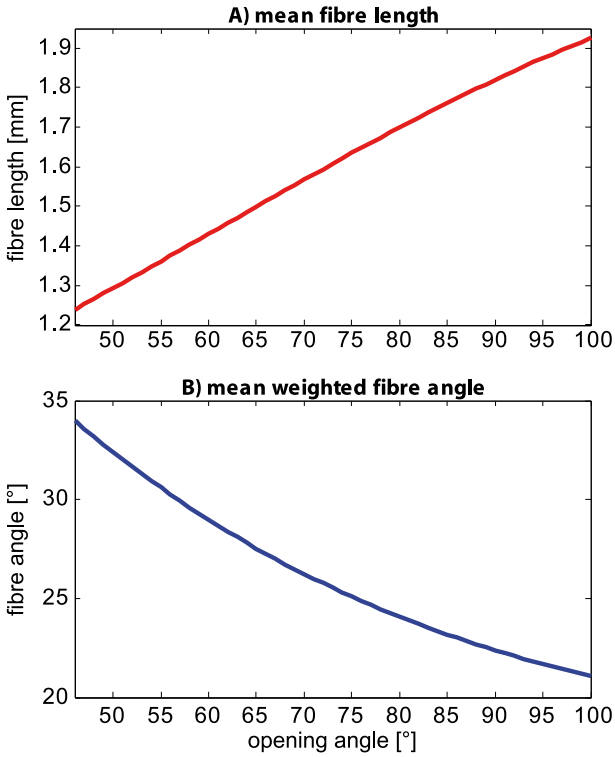

Fig. 3. Changes of **A**: the mean fibre length and **B**: the mean fibre angle of the mandibular adductor muscle of *Periplaneta americana* for the mandible opening angles between 48° and 100°.

fibre angle changes from about 31° to 23°. The mean fibre length increases nearly linearly from 1.24 mm with closed mandibles to 1.93 mm at 100° mandible opening. In the range from 55° to 85°, the fibre length changes from about 1.36 mm to 1.76 mm; this corresponds to a relative increase of 35% and 23%, respectively. Fibre length and opening angle are almost linearly related. Thus, the ascending limb of the relationship of bite force and opening angle, which occurs between 55° and 62° corresponds to a mean muscle fibre length range from 1.36 mm to 1.46 mm (Fig. 3). The force plateau, between 62° and about 75° (Weihmann et al. in press), corresponds to fibre lengths from 1.46 mm to 1.63 mm and the descending limb to fibre length between 1.63 mm and about 1.76 mm (Fig. 3).

Muscle pennation results in muscle fibre stresses higher than whole muscle stresses (Paul & Gronenberg 1999). According to its dependency on the cosine of the pennation angle, the differences are larger the higher the muscle pennation angle. The pennation of mandibular adductors is maximal when the mandibles are closed and decreases with increasingly opened mandibles. Thus, muscle fibre stress is up to 20% higher than whole muscle stress when mandibles are closed and the mean pennation angle gains its maximum value of 34°. At maximally opened mandibles, the mean pennation angle is only about 21° and the surplus in fibre stress, thus, is only about 7%. In the range from 55° to 85° mandible opening, the pennation decreases from 31° to 23° which results in fibre stress values exceeding that of the whole muscle by about 17% and 9% respectively.

Table 3. Distances in the mandibles of *Periplaneta americana*. — ***Abbreviations***: il = inner lever i.e. distance between joint axis and tendon attachment; ol1–ol4 = outer lever i.e. distances between joint axis and the mandible teeth 1 to 4 (distal to proximal).

	right		left	
	mean	std	mean	std
il [mm]	0.92	±0.06	0.92	±0.09
ol1 [mm]	2.52	±0.13	2.52	±0.10
ol2 [mm]	2.33	±0.11	2.36	±0.12
ol3 [mm]	1.98	±0.09	2.32	±0.10
ol4 [mm]	-	-	1.94	±0.10

Table 4. Angles between the inner lever (il) and outer levers (ol) for all incisivi of *Periplaneta americana*.

	right		left	
	mean	std	mean	std
∠il-ol1 [°]	49.9	±1.3	49.3	±1.8
∠il-ol2 [°]	42.8	±2.9	47.0	±2.2
∠il-ol3 [°]	39.0	±2.4	39.1	±2.2
∠il-ol4 [°]	-	-	36.9	±2.4

4. Discussion

The mouthparts of *P. americana*, especially the mandible, and its mechanics were the focus of recent studies (Schmitt et al. 2014; Weihmann et al. 2015; Weissing et al. in press). Their mandibles are roughly triangular cutting devices. In contrast to mechanical shears and scissors their mechanics are characterized by two independent joint axes such that there is usually no point of intersection if the animal grasps a piece of food. On the contrary, the cutting edges of the two mandibles are typically divided by a relatively wide spacing. While only the distal parts of the mandibles are characterised by sharp edges and teeth, the more proximal parts, i.e. those which could, in principle, make up a point of contact between the opposed mandibles, are blunt and not suitable to generate shear forces. Thus, the mechanism of cockroach mandibles is rather analogous to staggered pairs of parrot beak pruners. Initially, the tips of the mandible teeth perforate the outer surface of a food item and then the proximal edges of the teeth cut apart the material (see Figs. 1, 2) cut apart the material. Only when the opening angles of the mandibles are small, the cutting edges of some teeth can interact like scissor blades and may generate significant shear forces. Here, particularly the second right and the third left teeth seem to have the capacity to form a structure similar to the carnassial structure of carnivore mammals enabling *P. americana* to cut up stringy matter such as fibrous plant and animal materials.

P. americana, as many other roaches, is an omnivorous insect (Bell et al. 2007). This diet is also reflected in their mandibular apparatus. Each mandible has distal incisivi as well as a proximal grinding area, the mola (Fig. 1A,B; Weissing et al. in press). Carnivorous insects such as dragonflies or mantids lack the mola and therefore have a mesal cutting edge (Blanke et al. 2012; Wipfler et al. 2012) while the mesal side of the mandible of herbivorous insects contains a sole grinding area (e.g. Friedemann et al. 2012).

Adaptations towards the generalized lifestyle can also be found in the mean fibre angle of the mandibular adductor. For adductors with elongated apodemes and only little horizontal width, Paul & Gronenberg (1999) proposed a geometrical model. It predicts that for maximum bite force generation the optimum fibre angle is 45° whereas maximum closing velocities are reached with fibres aligned along the force direction. Thus, most insect species should adopt muscles with intermediate fibre angles. With 34° at closed mandibles, the mean fibre angle in *P. americana* is similar to many non-specialized ants (Paul & Gronenberg 1999). In contrast, the fibre angles are as small as 15° in fast predatory ants while muscle fibres in herbivorous, leaf-cutter and seed eating ants attach at angles steeper than 40° (Paul & Gronenberg 1999). Although most literature refer to measurements with closed mandibles, from a functional point of view, fibre angles should be obtained at the force plateau of a mandibular adductor. In *P. americana* this plateau is reached at mandible opening angles between 62° and 75° (Weihmann et al. 2015). Here, the mean fibre angles are smaller and reach angles between 25° and 28°.

A small mechanical advantage (MA), i.e. the quotient of the inner lever to the outer lever results in a smaller force output in the mandible. However, the potential maximum velocity of the mandible tip increases and the time necessary to close the mandibles decreases. Accordingly, the detritivore larva of the beetle *Liocola* exhibits a rather high MA of 0.54 (Gorb & Beutel 2000). The mandibles of predatory aquatic beetle larvae of the species *Hydrophilus* and *Cybister*, which in turn rely on fast attacks on rather soft-bodied prey are comparatively slender and have MA values of 0.28 and 0.26 respectively (Gorb & Beutel 2000). Additionally, the mandibles of *Hydrophilus* larvae have a prominent cutting ridge (retinaculum) at their median central part, which allows the cracking of snail shells by taking advantage of the much higher mechanical advantage (Gorb & Beutel 2000). Male stag beetles (Goyens et al. 2014), which use their elongated mandibles in their notorious fights for mating opportunities have also the need for fast actions. Thus, depending on the bite positon, MA values of male mandibles range

from 0.13 to 0.28, while the MA of female mandibles is about 0.34. In carnivorous ground and rove beetles MA values range between 0.35 and 0.59 (Wheater & Evans 1989) and 0.18 and 0.46 (Li et al. 2011) respectively. Both examinations present the MA of the distal most teeth of the mostly single-toothed predatory mandibles. Similar values are measured in *Periplaneta americana.* They range from 0.37 to 0.47 from the distal most to the proximal incisivi with 0.39 in the second right and third left which are the strongest teeth. Thus the omnivorous lifestyle of *Periplaneta americana* is not reflected in the mechanical advantage.

With closed mandibles, the position of the inner lever almost coincides with the horizontal line, i.e. the line between the two anterior condyles. Therefore, the force of the adductor muscle is optimally transmitted to the mandibles' teeth and edges in this condition. However, the orientation of the single muscle fibres may deviate significantly from the current direction of the main muscle force. In the transverse plane the fibre angles of the bundles *f* and *a* deviate up to 60° from each other (Figs. 1, 2). Therefore, depending on the opening angle of the mandibles, differential or sequential activation patterns are conceivable, i.e. lateral bundles are active primarily when opening angles are small and medial fibre bundles show highest activity when opening angles are high. However, it has been previously found in ants (Paul & Gronenberg 2002) that posterior and lateral fibres are probably not recruited differentially, although fast muscle fibres, lumped together in specific muscle subunits, can be activated independently.

Most of the fibre bundles gain attachment area and therefore effective cross-sectional area by spreading out in anterio-posterior direction at the curved dorsal wall of the head capsule (Fig. 2B). In this way, the attachment areas largely match the effective cross-sectional areas. Only bundle *b* and *h* attach almost exclusively at the posterior wall of the head capsule. Their attachment areas are significantly larger than the cross-sectional areas. Accordingly, the forces generated by these muscle bundles are distributed over a relatively larger area and this decreases the tensile loading of the comparatively flat posterior wall of the head capsule, which probably is not optimised to withstand high tensile forces.

The maximum bite force of *P. americana* is about 0.5 N (Weihmann et al. 2015). However, this study used a 2D-force sensor which allowed only for the discrimination of medio-lateral and dorso-ventral bite forces. Anterio-posterior force components could not be resolved. Though the movability of the mandibles is largely restricted to the transverse plane, the joint axes of the mandibles are tilted with regard to the length axis of the head by about 17°. Consequently, and according to trigonometric functions, absolute mandible forces were up to 6% higher than the measured resulting forces. Thus, muscle forces and stresses might also be higher. In contrast to the tilted joint axes, the blades and cutting edges of the mandibles are almost aligned in parallel to the transverse plane. The anterio-posterior force components, therefore, primarily seem to facilitate shovelling of the reduced food towards the oesophagus and do not contribute to the biting forces themselves.

If applying the log10 transformation of the bite force quotient (BFQ), i.e. maximum bite force/body weight$^{0.66}$ as suggested by van der Meijden et al. (2012), the resulting logBFQ is 0.99 for *P. americana*. This quotient should be independent of body mass and therefore allow comparisons between different sized animals (van der Meijden et al. 2012). Male stag beetles of the species *Cyclommatus metallifer* can generate bite forces of up to 9 N with a body mass of about 1.36 g (Goyens et al. 2014) which results in logBFQ of 2.19. Even higher values can be expected for leaf-cutter ants. With an estimated bite force of more than 1 N (Weihmann et al. 2015, supporting information: S1 Text) and a body mass of about 20 mg, the ants' logBFQ exceeds 2.45. Thus, insects with specialized mandibular apparatus that allow them to clutch opponents or cut tough leaves exhibit much higher values than omnivorous *P. americana*. For chelate crustaceans, scorpions and solpugids the values range from 0.98 to 2.96, where the highest values were attained in crustaceans (Taylor 2000; van der Meijden et al. 2012). Apparently insects, arachnids and crustaceans include species with moderate to very distinct biting abilities. However, a comparison between insects and crustaceans is difficult since all crustaceans studied so far use their chelae rather than their mandibles to crush prey. Moreover available literature mostly refers to species specialised for slow and hard-shelled prey. Thus their bite forces are expected to be above non-specialist species (van der Meijden et al. 2012; Taylor 2000). Crustaceans are arguably the most morphologically diverse group of arthropods, but the species studied so far do not reflect this actual biodiversity. From a phylogenetic point of view, insects are in fact a terrestrial group of crustaceans (e.g. Misof et al. 2014). In contrast to chelae, mandibles are independently driven and work against each other. However, according to Newton's 3rd law, one moveable lever with only one adductor acting against a rigid counterpart, in principle, can apply the same biting force as mandibles of the same size with equally sized adductors. The advantages of two independently driven blades seems not to primarily be to increase bite force but rather reduce length changes of the adductors when the animals encompass and cut food pieces of a certain size. That is because the working ranges of both sides add up, and high opening angles can be achieved with only half the muscular length change. As a consequence, the adductors can act closer to their optimum length of 1.46 mm to 1.63 mm in *P. americana* (Weihmann et al. 2015), which results in increased efficiency. Moreover, the effective closing velocity is higher for a given mean sarcomere and fibre length because the velocities of both sides also add up. If no particularly fast actions are needed, the muscles can still act closer to isometric conditions, which increases the maximum biting force or efficiency again (Hill 1938; Wendt & Gibbs 1974; Crow & Kushmerick 1982).

Table 5. Volume of the head capsule (in mm^3), and the fibres and tendon of the mandible adductor (M. craniomandibularis internus, 0md1) and abductor muscles (M. craniomandibularis externus, 0md3) of selected species. The muscle volumes are provided in absolute values (mm^3) and as percentage of the volume of the head capsule.

Species	head capsule [mm^3]	0md1 [mm^3]	0md1 [%]	0md3 [mm^3]	0md3 [%]	0md1 / 0md3
Blattodea / *Periplaneta americana*	45.44 ± 3.43	6.64 ± 1.71	14.61	0.79 ± 0.07	1.74	8.41
Blattodea / *Ergaula* sp.	9.67	1.15	11.90	0.08	0.87	14.37
Blattodea / *Salganea* sp.	14.84	4.44	29.93	0.25	1.66	18.07
Blattodea / *Mastotermes darwiniensis*	9.62	2.54	26.43	0.23	2.35	11.26
Mantodea / *Hymenopus coronatus*	42.43	6.99	16.48	0.80	2.12	8.74
Grylloblattodea / *Galloisiana yuassai*	5.10	1.08	21.12	0.09	1.67	12.62
Phasmatodea / *Phyllium siccifolium*	10.43	3.01	28.84	0.13	1.24	23.19
Phasmatodea / *Timema* sp.	13.19	2.51	19.02	0.12	0.93	20.36

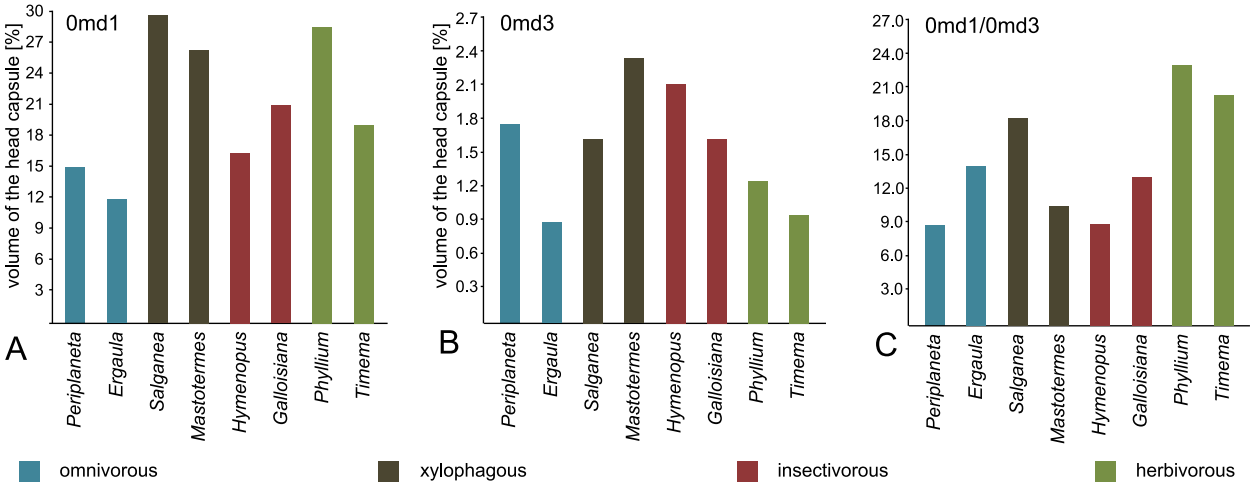

Fig. 4. Relative volume of the mandibular muscles for selected species of insects. **A**: relative volume of M. craniomandibularis internus (0md1) compared to the volume of the head capsule; **B**: relative volume of M. craniomandibularis externus posterior (0md3) compared to the volume of the head capsule; **C**: ratio between M. craniomandibularis internus (0md1) and M. craniomandibularis externus posterior (0md3).

The rather low maximum bite forces exerted by *P. americana* are also reflected by the relative small volume of the adductor muscles relative to the head capsule (Table 5; Fig. 4). In the three studied specimens of *P. americana*, the mandible adductors represented about 14.6% ± 3.8% of the entire volume of the head capsule. The only lower value (11.9%) was observed in the likewise omnivorous cockroach *Ergaula* sp. With the exception of the mantid *Hymenopus coronatus* (16.5%), all other species studied here have distinctly higher values. In *Hymenopus* this low value might be a result of the large dorsal fastigium and the cone-like compound eyes which strongly increase the volume of the head capsule (WIPFLER et al. 2012). In our study, the highest values were found in the wood-feeding cockroach *Salganea* sp. (29.9%) and the herbivorous phasmatodean *Phyllium siccifolium* (28.8%). However, quite similar values were documented for carnivorous rove beetles (LI et al. 2011). They seem to also have relatively big mandibular adductor muscles making up about 26% to 33% of the head capsule's volume. Even larger muscles were found in ant workers (PAUL 2001), where the adductors can occupy up to 66% of the head capsule volume.

The ratios between the volumes of the adductor and the abductor muscle varied considerably between differently adapted species. Higher ratios seem to be reserved for species specialised in tough food. We observed the highest ratio in the herbivorous phasmatodeans (23.2 in *Phyllium* and 20.4 in *Timema*) followed by the xylophagous roach *Salganea* (18.1). Relatively low ratios of 8.4 were found in *P. americana* (Fig. 3) and 8.7 in the insectivorous mantid. Since lower ratios and accordingly relatively stronger mandible abductor muscles might facilitate higher rates when repeated biting is required, or faster reopening when a predatory strike missed, this feature is probably particularly useful in species with a diet comprising a significant part of elusive animal source food. In the omnivorous roach *Ergaula* as well as the xylophagous and herbivours species the adductor is at least 11 times bigger than the abductor. LI et al. (2011) found

volume ratios between 6.3 and 12.2 in three species of predatory rove beetles with distinctly differing mandible morphologies.

It should be kept in mind that the specimens of *P. americana* used in this study were bred for several generations and fed with uniform diet. However, the same applies to the cockroach *Ergaula* sp., the mantid *Hymenopus coronatus* and the phasmatodean *Phyllium siccifolium,* while the other species were taken from the wild. The effects of uniform diet and constant inbreeding on the development of the chewing apparatus and other organs have to be clarified by future analysis but we assume that they are detrimental for normal development.

The chewing apparatus of insects is a complex structure allowing for both, hard biting, shredding tough food items, and grinding up smaller pieces. In *P. americana* like in other dicondylic insects, chewing is largely driven by the structurally complex mandibular adductor muscle. In *P. americana* it consist of eight distinct muscle fibre bundles. These bundles, in turn, consist of muscle fibres with variable lengths and fibre angles. Additionally, they are most likely composed of different fibre types (Paul & Gronenberg 1999, 2002). The small relative muscle size and intermediate fibre angle both reflect these cockroaches' omnivorous life style while the mechanical advantage seems not a good predictor.

5. Acknowledgments

We thank Tobias Siebert (Stuttgart) for interesting discussions of the specific muscle structure. We thank Hans Pohl (Jena) for creating the outstanding illustration of the coordinate system (Fig. 1D) and Aleksandra Birn-Jeffery (Cambridge) for proof-reading the draft. This work was financially supported by the German Research Foundation (DFG) [We 4664/2-1 to TW, WI 4324/1-1 to BW, and KL 2707/2-1 to TK] and by a PostDoc stipend of the Daimler und Benz Stiftung (32-10/12 to BW).

6. References

Ahn A.N., Full R.J. 2002. A motor and a brake: two leg extensor muscles acting at the same joint manage energy differently in a running insect. – Journal of Experimental Biology **205**(Pt 3): 379–389.

Bell W.J., Roth L.M., Nalepa C.A. 2007. Cockroaches: ecology behaviour, and natural history. – The Johns Hopkins University Press: Baltimore. 230 pp.

Bennet-Clark H.C. 1975. The energetics of the jump of the locust *Schistocerca gregaria*. – Journal of Experimental Biology **63**(1): 53–83.

Blanke A., Wipfler B., Letsch H., Koch H., Beckmann F., Beutel R., Misof B. 2012. Revival of Palaeoptera – head characters support a monophyletic origin of Odonata and Ephemeroptera (Insecta). – Cladistics **28**(6): 560–581.

Chapman R.F., de Boer G. 1995. Regulatory Mechanisms in Insect Feeding. – Springer: Heidelberg.

Clissold F.J. 2007. The biomechanics of chewing and plant fracture: mechanisms and implications. – Advances in Insect Physiology **34**: 317–372.

Crow M.T., Kushmerick M.J. 1982. Chemical energetics of slow- and fast-twitch muscles of the mouse. – The Journal of General Physiology **79**(1): 147–166.

Friedemann K., Wipfler B., Bradler S., Beutel R.G. 2012. On the head morphology of *Phyllium* and the phylogenetic relationships of Phasmatodea (Insecta). – Acta Zoologica **93**: 184–199.

Friedrich F., Matsumura Y., Pohl H., Bai M., Hörnschemeyer T., Beutel R.G. 2014. Insect morphology in the age of phylogenomics: innovative techniques and its future role in systematics. – Entomological Science **17**: 1–24.

Gorb S.N., Beutel R.G. 2000. Head-capsule design and mandible control in beetle larvae: A three-dimensional approach. – Journal of Morphology **244**: 1–14.

Goyens J., Dirckx J., Dierick M., Van Hoorebeke L., Aerts P. 2014. Biomechanical determinants of bite force dimorphism in *Cyclommatus metallifer* stag beetles. – Journal of Experimental Biology **217**(Pt 7): 1065–1071.

Grimaldi D., Engel M.S. 2005. Evolution of the Insects. – Cambridge University Press: New York.

Hill A.V. 1938. The heat of shortening and the dynamic constants of muscle. – Proceedings of the Royal Society of London B: Biological Sciences **126**(843): 136–195.

Jahromi S., Atwood H. 1969. Correlation of structure, speed of contraction, and total tension in fast and slow abdominal muscle fibers of the lobster (*Homarus americanus*). – Journal of Experimental Zoology **171**(1): 25–37.

Ker R.F., Alexander R.M., Bennett M.B. 1988. Why are mammalian tendons so thick? – Journal of Zoology **216**(2): 309–324.

Li D., Zhang K., Zhu P., Wu Z., Zhou H. 2011. 3D configuration of mandibles and controlling muscles in rove beetles based on micro-CT technique. – Analytical and Bioanalytical Chemistry **401**(3): 817–825.

Maier L., Root T.M., Seyfarth E.A. 1987. Heterogeneity of spider leg muscle: Histochemistry and electrophysiology of identified fibers in the claw levator. – Journal of Comparative Physiology B: Biochemical, Systemic, and Environmental Physiology (Historical Archive) **157**(3): 285–294.

Misof B., Liu Sh., Meusemann K., Peters R.S., Donath A., Mayer C., Frandsen P.B., Ware J., Flouri T., Beutel R.G., Niehuis O., Petersen M., Izquierdo-Carrasco F., Wappler T., Rust J., Aberer A.J., Aspöck U., Aspöck H., Bartel D., Blanke A., Berger S., Böhm A., Buckley T., Calcott B., Chen J., Friedrich F., Fukui M., Fujita M., Greve C., Grobe G., Gu Sh., Huang Y., Jermiin L.S., Kawahara A.Y., Krogmann L., Kubiak M., Lanfear R., Letsch H., Li Y., Li Zh., Li J., Lu H., Machida R., Mashimo Y., Kapli P., McKenna D.D., Meng G., Nakagaki Y., Navarrete-Heredia J.L., Ott M., Ou Y., Pass G., Podsiadlowski L., Pohl H., Reumont B.M. v., Schütte K., Sekiya K., Shimizu Sh., Slipinski A., Stamatakis A., Song W., Su X., Szucsich N.U., Tan M., Tan X., Tang M., Tang J., Timelthaler G., Tomizuka Sh., Trautwein M., Tong X., Uchifune T., Walzl M.G., Wiegmann B.M., Wilbrandt J., Wipfler

B., Wong T.K.F., Wu Q., Wu G., Xie Y., Yang Sh., Yang Q., Yeates D.K., Yoshizawa K., Zhang Q., Zhang R., Zhang W., Zhang Y., Zhao J., Zhou Ch., Zhou L., Ziesmann T., Zou Sh., Li Y., Xu X., Zhang Y., Yang H., Wang J., Wang J., Kjer K.M., Zhou X. 2014. Phylogenomics resolves the timing and pattern of insect evolution. – Science **346**: 763–767.

Paul J. 2001. Mandible movements in ants. – Comparative Biochemistry and Physiology Part A: Molecular & Integrative Physiology **131**(1): 7–20.

Paul J., Gronenberg W. 1999. Optimizing force and velocity: mandible muscle fibre attachments in ants. – Journal of Experimental Biology **202**(7): 797–808.

Paul J., Gronenberg W. 2002. Motor control of the mandible closer muscle in ants. – Journal of Insect Physiology **48**(2): 255–267.

Schmitt C., Rack A., Betz O. 2014. Analyses of the mouthpart kinematics in *Periplaneta americana* (Blattodea, Blattidae) using synchrotron-based X-ray cineradiography. – Journal of Experimental Biology **217**(17): 3095–3107.

Seifert G. 1995. Entomologisches Praktikum. – Georg Thieme Verlag: Stuttgart, New York.

Siebert T., Weihmann T., Rode C., Blickhan R. 2010. *Cupiennius salei*: biomechanical properties of the tibia-metatarsus joint and its flexing muscles. – Journal of Comparative Physiolgy B **180**(2): 199–209.

Snodgrass R.E. 1944. The feeding apparatus of biting and sucking insects affecting man and animals. – Smithsonian Institution.

Taylor G.M. 2000. Maximum force production: why are crabs so strong? – Proceedings of Biological Science **267**(1451): 1475–1480.

van der Meijden A., Coelho P.L., Sousa P., Herrel A. 2013. Choose your weapon: defensive behavior is associated with morphology and performance in scorpions. – PloS one **8**(11): e78955.

van der Meijden A., Langer F., Boistel R., Vagovic P., Heethoff M. 2012. Functional morphology and bite performance of raptorial chelicerae of camel spiders (Solifugae). – Journal of Experimental Biology **215**(Pt 19): 3411–3418.

Weihmann T., Reinhardt L., Weissing K., Siebert T., Wipfler B. 2015. Fast and powerful: Biomechanics and bite forces of the mandibles in the American cockroach *Periplaneta americana*. – PlosOne.10(11): e0141226.

Weihmann T., Goetzke H.H., Günther M. in press. Requirements and limits of anatomy-based predictions of locomotion in terrestrial arthropods with emphasis on arachnids. – Journal of Paleontology.

Weissing K., Klass K.-D., Weihmann T., Wipfler B. in press. The cephalic morphology of the American roach *Periplaneta americana* (Blattodea). – Arthropod Systematics & Phylogeny.

Wendt I.R., Gibbs C.L. 1974. Energy production of mammalian fast- and slow-twitch muscles during development. – American Journal of Physiology **226**: 642–647.

Wheater C.P., Evans M.E.G. 1989. The mandibular forces and pressures of some predacious Coleoptera. – Journal of Insect Physiology **35**(11): 815–820.

Wipfler B., Machida R., Müller B., Beutel R.G. 2011. On the head morphology of Grylloblattodea (Insecta) and the systematic position of the order, with a new nomenclature for the head muscles of Dicondylia. – Systematic Entomology **36**: 241–266.

Wipfler B., Wieland F., DeCarlo F., Hörnschemeyer T. 2012. Cephalic morphology of *Hymenopus coronatus* (Insecta: Mantodea) and its phylogenetic implications. – Arthropod Structure & Development **41**(1): 87–100.

Wipfler B., Klug R., Ge S.-Q., Bai M., Göbbels J., Yang X.-K., Hörnschemeyer T. 2015. The thorax of Mantophasmatodea, the morphology of flightlessness, and the evolution of the neopteran insects. – Cladistics **31**: 50–70.